

Thermal Behaviour of Recurring Slope Lineae Areas in Palikir Crater

Cédric Millot (1), Cathy Quantin-Nataf (1), Cédric Leyrat (2) and Matthieu Volat (1)
(1 Laboratoire de Géologie de Lyon : Terre, Planète, Environnement, UMR CNRS 5276 (CNRS, ENS, Université Lyon1), Université Claude Bernard, Lyon1, France (2) Observatoire de Paris, CNRS UMR 8109, Université PSL, Sorbonne Université, Université Paris-Diderot | (cedric.millot@ens-lyon.fr).

1. Introduction

Recurring Slope Lineae (RSL) are seasonal streaks that occur each year at low albedo sites on warm steep slopes on Mars and fade or disappear during cold seasons [1]. They are of particular interest since their characteristics questions the possible presence of liquid water on present-day at the surface of Mars. Hence, several studies have interpreted RSL as freshwater flows [1] [2]. Alternative source mechanisms for RSL have been discussed requiring liquid water such as brines [3], subsurface aquifers [4], or dry mechanisms like wind-induced flows [5] or gas-triggered flows [6]. To date, liquid water has not been observed and the presence of deliquescent salts (perchlorates [7]) is still debated on RSL sites [5]. As RSL occur on warm seasons, surface and subsurface temperatures assessments seem to be essential to fully understand the RSL nature. Hence, temperature computations on various locations where RSL appear will provide valuable information about the thermal state of the ground. We focus on a well-documented RSL region in south hemisphere, Palikir Crater [1] (figure 1), to provide quantitative estimations of RSL length variations. We study the effects of seasons on the incoming solar energy at the surface and subsurface temperatures through a numerical thermal model [8] [9] to finally retrieve spatial variations of temperatures as a function of location on Mars, slope orientation or time at HiRISE scale. In the end, thermal models provide valuable constraints on temperature range where RSL occur and allow narrow possible source mechanisms.

2. Methods

We use HiRISE imagery [10] and the associated Digital Elevation Models (DEM) products to work with the highest spatial resolution available (25 cm/pixel for HiRISE pictures; 1 m/pixel for HiRISE DEM [11]). Such spatial resolution is required to solve the RSLs of which width is typically from a meter to few meters. HiRISE images and HiRISE

DEM are included in GIS software to assess local slopes, orientations and elevations using. Regions Of Interest (ROIs) are mapped to contour the source region of RSL using ArcGIS toolbox (blue area in figure 1). These ROIs are the geometrical data entered into our thermal model. Sites with a temporal survey over a full seasonal cycle are chosen preferentially. We focus in this paper on one particular site: Palikir Crater located in mid-southern latitudes (41.6°S, 202.3°E).

2.1. RSL length measurements

In order to survey the evolution of the length of RSLs through the seasonal cycle, recurrent streaks are identified and measured using HiRISE images using GIS tool. Then, we compute the mean streak value for each HiRISE picture. Mean length seasonal variations are then compared with numerically computed surface and subsurface temperatures.

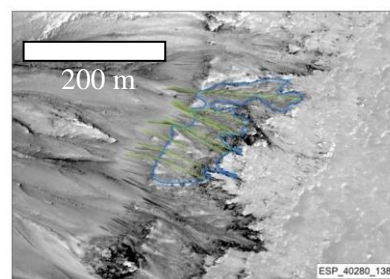


Figure 1: RSL area in Palikir Crater during southern summer ($L_S = 300.03^\circ$, ESP_040280_1380). RSL source area has been delimited using the blue area on which we extract pixel by pixel the elevations, slopes and orientations. The green lines map the dark slope lineae.

2.2. Thermal model

We use a thermal model which computes insolation (= incoming solar flux at the surface) and surface and subsurface temperatures [9] of the ground to constrain the possible mechanisms at the origin of these seasonal processes. The model has been apply to each pixel of the extracted DEMs within the RSL

source region we map. The DEM provides the slope, orientations and elevations which allows to compute the insolation for each pixel. The incidence angle (angle between sunrays and the normal to the local surface) is calculated for every time step involving SPICE/NAIF libraries [12]. Then, the incoming energy is calculated thanks to this angle and Mars orbital parameters provided by SPICE/NAIF data at every time step. Insolations are then used in a thermal model, MarsTHERM [8] which has been modified to take our insolation map as inputs [9]. Taking into account the effects of heat conduction in depth, CO₂ condensation-sublimation cycle or planetary surface reemission, MarsTHERM computes surface and subsurface temperatures for all DEM pixels at any time for a complete martian year. We can then produce temperature maps at the surface or at few meters depth as well as vertical temperature profiles for a given point. Temperature computations are performed for a bolometric albedo $A_b = 0.10$ and a thermal inertia $I = 400$ tiu (thermal inertia units, [13]), which corresponds to a mixing of sand and more indurated material, typical of RSL sites [14].

3. Results

9 streaks are measured in Palikir Crater for a given RSL area using 27 HiRISE ortho-images. RSL morphology changes are visible for more than three consecutive Martian Years (MY), from MY28 to MY31. The mean length streaks value for each image is calculated to give the seasonal length profiles. The profile in figure 2 describes the mean length of the considered streaks in Palikir Crater. HiRISE imagery highlights a sharp increase in streaks lengths at a solar longitude (L_S) around $L_S = 250^\circ$ for every studied MY, from 0 to 180 m in average. Slight differences in length can be observed between different MY for the same epoch of the year. Indeed, MY29 and MY31 differ from MY30 around $L_S = 330^\circ$ which shows lower lengths than MY29 and MY31. RSL then start their fading in early fall, when L_S is between 0 and 45° until the southern winter (after $L_S = 90^\circ$) where RSL are completely faded. Figure 3 represents the mean surface temperature computed for the exact local hour and L_S of the 27 studied HiRISE pictures. Surface temperatures computed for every pixel are spatially averaged to produce a mean surface temperature for the entire ROI. Hence, 27 mean temperatures (in K) form the temperature profile in figure 3 (in blue). Red dots represent spatial variances within the ROI. Temperature profile is consistent with seasons; in

other words, high temperatures are synchronous with perihelion ($L_S = 250^\circ$) and summer in south hemisphere (summer starts at $L_S = 270^\circ$) and low temperatures with winter and aphelion. Surface temperatures reach 296 K and decrease to 230 K for the set of parameters we use here.

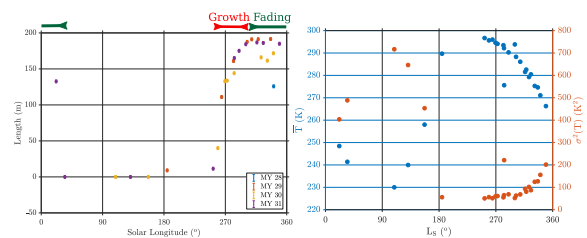


Figure 2: Left: Mean length temporal profile during four consecutive martian years (MY). The profile shows a sharp increase in length at $L_S = 250-290^\circ$, during southern summer. RSL fades during early fall, between $L_S = 0^\circ$ and $L_S = 45^\circ$. Notice that fading is progressive and the moment when RSL is considered completely faded (average length equal to 0 m) depends on the observer. Right: Temperature profile (in blue) and variance (in red) for RSL area.

RSL fading occurs around $L_S = 300-310^\circ$, where surface temperatures are still well above 273 K. Our results highlight that temperature superior to the pure water melting point is not a sufficient condition for the sustainability of RSL.

4. Conclusion

New assessments of thermal state of RSL surroundings have been done for Palikir Crater RSL site. Our study suggests the length increase during warm seasons, where surface temperature exceeds 290 K, and start to decrease before the temperature drop below 290 K. This range of temperatures is at first order consistent with several proposed mechanisms, including freshwater or brines [4] [7], but do not fully explain the observed seasonality, especially during RSL fading. Other RSL sites are under study to further constrain the surface temperatures when RSL starts to grow and fade at various ranges of orientations and latitudes.

[1] McEwen A. et al. (2011) *Science*, 333 (6043), 740-743 [2] McEwen A. et al. (2014) *Nature Geoscience*, 7(1), 53-58. [3] Gough R. et al. (2014) *Icarus*, 233, 316-327. [4] Stillman D. E. et al. (2017) *Icarus*, 285, 195-210. [5] Vincendon M. et al. (2019) *Icarus*, 325, 115-127. [6] Schmidt F. et al. (2017) *Nature Geoscience*, 10(4), 270-273. [7] Ojha L. et al. (2015) *Nature Geoscience*, 8, 826-832. [8] Clifford S. M. and Bartels C. J. (1986) *LPSXVII*, 142-143 [9] Millot C. et al. (2018), LPSC XLIX, Abstract #2030. [10] McEwen A. et al. (2007) *JGR: Planets*, 112 (E5). [11] Kirk R. L. et al. (2008) *JGR*, 113. [12] Acton C. H. (1996) *Planetary and Space Science*, 44 (1), 65-70. [13] Putzig N.E. (2006), thesis. [14] Ojha L. et al (2014), *Icarus*, 231, 365-376.